Available online at www.sciencedirect.com
SCIENCE DIRECT®
Physics Letters A 335 (2005) 383–393
PHYSICS LETTERS A
www.elsevier.com/locate/pla

Dynamical mechanism for band-merging transitions in quasiperiodically forced systems

Woochang Lim, Sang-Yoon Kim *

Department of Physics, Kangwon National University, Chunchon, Kangwon-Do 200-701, South Korea

Received 22 September 2004; received in revised form 1 December 2004; accepted 3 December 2004

Available online 29 December 2004

Communicated by C.R. Doering

Abstract

As a representative model for quasiperiodically forced period-doubling systems, we consider the quasiperiodically forced logistic map, and investigate the mechanism for the band-merging transition. When the smooth unstable torus loses its accessibility from the interior of the basin of an attractor, it cannot induce the "standard" band-merging transition. For this case, we use the rational approximation to the quasiperiodic forcing and show that a new type of band-merging transition occurs for a nonchaotic attractor (smooth torus or strange nonchaotic attractor) as well as a chaotic attractor through a collision with an invariant ring-shaped unstable set which has no counterpart in the unforced case. Particularly, a two-band smooth torus is found to transform into a single-band intermittent strange nonchaotic attractor via a new band-merging transition, which corresponds to a new mechanism for the appearance of strange nonchaotic attractors. Characterization of the intermittent strange nonchaotic attractor is made in terms of the average time between bursts and the local Lyapunov exponents.

PACS: 05.45.Ac; 05.45.Df; 05.45.Pq

Keywords: Quasiperiodically forced systems; Band-merging transition

1. Introduction

Dynamical transitions of attractors which occur with variation of the system parameters have been a topic of considerable interest [1]. Particularly, chaotic transitions attracted much attention. In a large class of dissipative dynamical systems, a chaotic attractor appears via a period-doubling cascade when a nonlinearity parameter a passes a threshold value [2]. Beyond the critical value of a, successive band-merging (BM) transitions of the chaotic attractor occur through collision with unstable periodic orbits [3]. These BM transitions in period-doubling systems are well studied.

* Corresponding author.
E-mail addresses: wclim@kwnu.kangwon.ac.kr (W. Lim), sykim@kangwon.ac.kr (S.-Y. Kim).

0375-9601/$ – see front matter
doi:10.1016/j.physleta.2004.12.057

Here, we are interested in the BM transitions in quasiperiodically forced systems driven at two incommensurate frequencies. These dynamical systems have received much attention because they typically have strange nonchaotic attractors (SNAs) that are geometrically strange (fractal) but nonchaotic (no positive Lyapunov exponent) [4]. Since the first suggestion of the existence of SNAs by Grebogi et al. [5], dynamical transitions in the quasiperiodically forced systems have been extensively investigated both theoretically [6–17] and experimentally [18]. There are some previous works related to the BM transitions. In the quasiperiodically forced logistic map, a transition from a period-doubled torus with two bands to a single-band SNA has been found to occur through a collision with the unstable parent torus [7]. In some case, the unstable parent torus becomes inaccessible from the interior of the basin of an attractor, and then it cannot induce any BM transition. Even for this case, BMs of smooth tori and SNAs were observed in other quasiperiodically forced systems [9,15]. However, the dynamical origin for this type of BM transitions remains unclear.

This Letter is organized as follows. In Section 2, we consider the quasiperiodically forced logistic map which is a representative model for quasiperiodically forced period-doubling systems, and investigate the dynamical mechanism for the BM transitions by varying the nonlinearity parameter a of the logistic map and the quasiperiodic forcing amplitude ε. For small ε, a standard BM transition of a chaotic attractor occurs through a collision with the smooth unstable torus which is developed from the unstable fixed point of the (unforced) logistic map. However, when ε passes a threshold value, a basin boundary metamorphosis occurs [19], and then the smooth unstable torus loses its accessibility from the interior of the basin of the attractor. For this case, the type of the BM transition changes. Using the rational approximations to the quasiperiodic forcing, it is found that a new type of BM transition occurs for a nonchaotic attractor (smooth torus or SNA) as well as a chaotic attractor via a collision with an invariant "ring-shaped" unstable set. Such a ring-shaped unstable set has no counterpart in the unforced case [17]. Particularly, for the case of a two-band smooth torus, the new BM transition results in the birth of a single-band intermittent SNA. This is a new mechanism for the appearance of SNAs. The intermittent SNA is also characterized in terms of the average time between bursts and the local Lyapunov exponents. As ε is further increased and passes another higher threshold value, the basin boundary metamorphosis no longer occurs, and then the smooth unstable torus regains its accessibility from the interior of the basin of the attractor. For this case, a standard BM transition of an attractor (smooth torus, SNA, or chaotic attractor) takes place again through a collision with the smooth unstable torus. (The BM transition in [7] corresponds to this standard transition.) Thus, the BM transition curve in the a–ε plane loses its differentiability at the two vertices bounding a segment on which a new type of BM transitions occur. We also note that this kind of new BM transitions occur through the same mechanism in typical quasiperiodically forced systems such as the quasiperiodically forced Hénon map and Toda oscillator [20]. Finally, a summary is given in Section 3.

2. Band-merging transitions in the quasiperiodically forced logistic map

We study BM transitions in the quasiperiodically forced logistic map M, which is often used as a representative model for the quasiperiodically forced period-doubling systems:

$$M: \quad \begin{cases} x_{n+1} = (a + \varepsilon \cos 2\pi\theta_n) x_n (1 - x_n), \\ \theta_{n+1} = \theta_n + \omega \ (\mathrm{mod}\, 1), \end{cases} \tag{1}$$

where $x \in [0, 1]$, $\theta \in S^1$, a is the nonlinearity parameter of the logistic map, and ω and ε represent the frequency and amplitude of the quasiperiodic forcing, respectively. This quasiperiodically forced logistic map M is noninvertible, because its Jacobian determinant becomes zero along the critical curve, $L_0 = \{x = 0.5,\ \theta \in [0, 1)\}$. Critical curves of rank k, L_k $(k = 1, 2, \ldots)$, are then given by the images of L_0, (i.e., $L_k = M^k(L_0)$; M^k is the kth iterate of M). Segments of these critical curves can be used to define a bounded trapping region of the phase space, called an "absorbing area", inside which, upon entering, trajectories are henceforth confined [21].

Here, we set the frequency to be the reciprocal of the golden mean, $\omega = (\sqrt{5} - 1)/2$. For the inverse golden mean, its rational approximants are given by the ratios of the Fibonacci numbers, $\omega_k = F_{k-1}/F_k$, where the sequence of $\{F_k\}$ satisfies $F_{k+1} = F_k +$

F_{k-1} with $F_0 = 0$ and $F_1 = 1$. Instead of the quasiperiodically forced system, we study an infinite sequence of periodically forced systems with rational driving frequencies ω_k. We assume that the properties of the original system M may be obtained by taking the quasiperiodic limit $k \to \infty$. Using this technique, the mechanism for the BM transitions is investigated.

Fig. 1(a) shows a phase diagram in the a–ε plane. Each phase is characterized by the Lyapunov exponent σ_x in the x-direction and the phase sensitivity exponent δ. The exponent δ measures the sensitivity with respect to the phase of the quasiperiodic forcing and characterizes the strangeness of an attractor in a quasiperiodically forced system [8]. A smooth torus with two bands which is born via a (first-order) torus doubling bifurcation of its parent torus with a single band exists in the region denoted by $2T$ and shown in light gray. It has a negative Lyapunov exponent ($\sigma_x < 0$) and no phase sensitivity ($\delta = 0$). When crossing the solid line (corresponding to a second-order torus doubling bifurcation line), the two-band torus becomes unstable and bifurcates to a four-band torus which exists in the region denoted by $4T$. Chaotic attractors with positive Lyapunov exponents ($\sigma_x > 0$) exist in the region shown in black. Between these regular and chaotic regions, SNAs that have negative Lyapunov exponents ($\sigma_x < 0$) and high phase sensitivity ($\delta > 0$) exist in the region shown in gray. Because of their high phase sensitivity, these SNAs have fractal structure [8]. A main interesting feature of the phase diagram is the existence of a second-order "tongue" that penetrates into the chaotic region. This tongue lies near the terminal point (denoted by the cross) of the second-order torus doubling bifurcation curve, as in the case of the main (first-order) tongue that exists near the terminal point of the first-order torus doubling bifurcation line (e.g., see Fig. 1(a) in [17]). For a clear view of the second-order tongue, the rectangular region in Fig. 1(a) is rotated and magnified in Fig. 1(b), using the new parameters, s_1 and s_2, defined by $s_1 = \cos(27^\circ)(a - 3.48) - \sin(27^\circ)(\varepsilon - 0.12)$ and $s_2 = \sin(27^\circ)(a - 3.48) + \cos(27^\circ)(\varepsilon - 0.12)$. Near this tongue, rich dynamical transitions such as BM transition (routes A, B, and C), intermittency (route a), and interior crisis (route b) occur through collision with an invariant ring-shaped unstable set which has no counterpart in

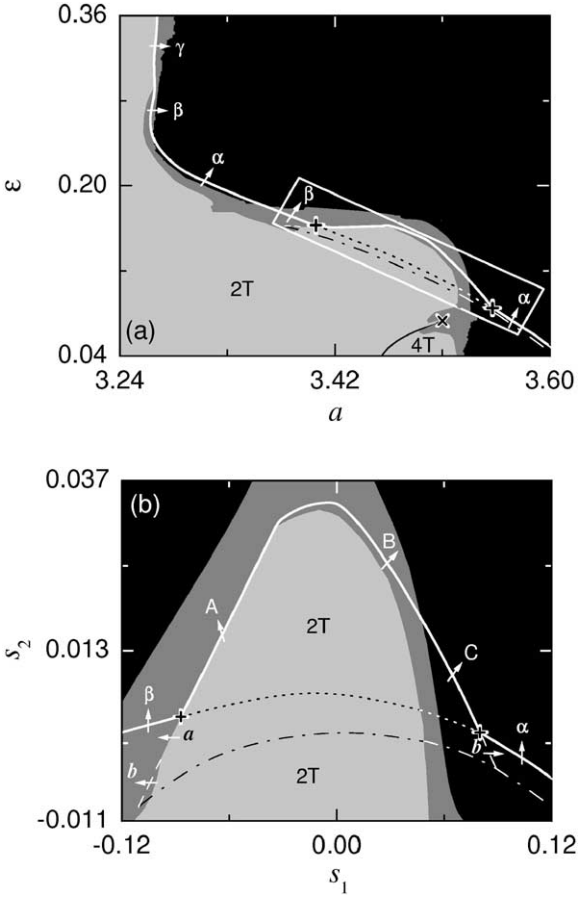

Fig. 1. (a) Phase diagram near the second-order tongue in the a–ε plane. Regular, chaotic, and SNA regimes are shown in light gray, black, and gray, respectively. For the case of regular attractor, tori with two and four bands exist in the regions denoted by $2T$ and $4T$, respectively. A second-order "tongue" that penetrates into the chaotic region lies near the terminal point (marked with the cross) of the second-order torus doubling bifurcation curve represented by the solid line. Through collision with the smooth unstable torus, standard BM transitions of a chaotic attractor, SNA, and smooth torus occur along the routes α, β, and γ, respectively. For a clear view of the tongue, the rectangular region is rotated and magnified in (b), using the new parameters s_1 [$\equiv \cos(27^\circ)(a - 3.48) - \sin(27^\circ)(\varepsilon - 0.12)$] and s_2 [$\equiv \sin(27^\circ)(a - 3.48) + \cos(27^\circ)(\varepsilon - 0.12)$]. A new type of dynamical transitions such as BM transition (routes A, B, and C), intermittency (route a), and interior crisis (route b) occur through collision with a ring-shaped unstable set born when passing the dash-dotted line. As the dotted line is crossed, a basin boundary metamorphosis occurs, and then the smooth torus becomes inaccessible from the interior of the basin of the attractor. Note that the BM transition curve, denoted by the white solid curve, is not differentiable at the two vertices, denoted by the pluses (+).

the unforced case. Here, we are interested in the BM transitions, which occur when crossing the white solid curve in Fig. 1.

We first consider a BM transition of a chaotic attractor which occurs along the route α ($\varepsilon = a - 3.55$) in Fig. 1(a). For this case, it is convenient to investigate the BM transition in M^2 (i.e., the second iterate of M). For $a = 3.596$ and $\varepsilon = 0.046$, there exists a two-band chaotic attractor with $\sigma_x = 0.159$ in the original map M. This chaotic attractor with two bands turns into a pair of conjugate chaotic attractors in M^2, which is denoted by black dots and bounded by the critical curves L_k ($k = 1, \ldots, 8$) in Fig. 2(a). The basins of the upper and lower chaotic attractors are shown in light gray and gray, respectively. A smooth unstable torus (denoted by the dashed line) lies on a basin boundary. As the parameters a and ε increase, the conjugate chaotic attractors become closer. Eventually, at a threshold value $(a, \varepsilon) = (3.600\,998, 0.050\,998)$, they contact the smooth unstable torus simultaneously, and merge to form a single chaotic attractor (i.e., an attractor-merging crisis occurs). Thus, for $a = 3.603$ and $\varepsilon = 0.053$, a single-band chaotic attractor with $\sigma_x = 0.196$ appears in M, as shown in Fig. 2(b). This BM transition corresponds to a natural generalization of the BM transition occurring for the unforced case ($\varepsilon = 0$). Hence, we call it the "standard" BM transition.

As ε is increased from zero, the standard BM transition curve in the a–ε plane continues smoothly. However, at a lower vertex $(a_l^*, \varepsilon_l^*) \simeq (3.552, 0.085)$ (denoted by a plus (+) in Fig. 1(a)), the standard BM transition curve ceases and a new type of BM transition curve begins by making a sharp turning. Hence, the BM transition curve is not differentiable at the vertex. For this case, beyond the vertex the standard BM transition curve is smoothly transformed into a curve of a basin boundary metamorphosis line denoted by a dotted line, while the new BM transition curve joins smoothly with an interior crisis line denoted by a dashed line at the vertex (see Fig. 1(b)). As the basin boundary metamorphosis line is passed, the basin boundary abruptly jumps in size [19], and when crossing the interior crisis line, a sudden widening of an attractor (without band merging) occurs. Note that these double (BM and interior) crises plus a basin boundary metamorphosis take place simultaneously at the vertex [22].

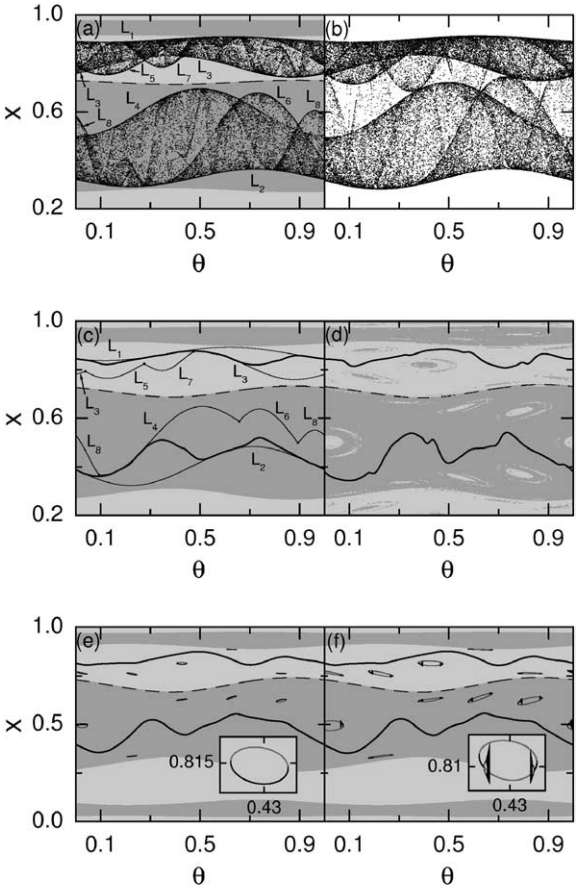

Fig. 2. (a), (b) Standard BM transition of a chaotic attractor. A two-band chaotic attractor in M turns into a pair of conjugate chaotic attractors in M^2. Such chaotic attractors, denoted by black dots and bounded by the critical curves L_k ($k = 1, \ldots, 8$), are shown in (a) for $a = 3.596$ and $\varepsilon = 0.046$. The basins of the upper and lower chaotic attractors are shown in light gray and gray, respectively. Through collision with the unstable smooth torus (denoted by a dashed line), the chaotic attractors merge to form a single chaotic attractor, as shown in (b) for $a = 3.603$ and $\varepsilon = 0.053$. (c) and (d) Basin boundary metamorphosis in M^2. (c) A pair of conjugate tori (denoted by heavy black lines) exists inside their absorbing areas bounded by L_k ($k = 1, \ldots, 8$) for $a = 3.46$ and $\varepsilon = 0.11$. (d) The basin of each torus contains "holes" of other basin of the counterpart for $a = 3.48$ and $\varepsilon = 0.13$ after breakup of the absorbing area. (e), (f) Appearance of ring-shaped unstable sets in the rational approximation of level 5 in M^2. A pair of conjugate ring-shaped unstable sets exists inside the basins of smooth tori (denoted by a black curve) for (e) $a = 3.396$ and $\varepsilon = 0.146$ and (f) $a = 3.4$ and $\varepsilon = 0.15$. Each ring-shaped unstable set is composed of F_5 ($= 5$) small rings. Magnified views of a ring are given in the insets. Note that each ring consists of the unstable part (composed of unstable orbits with the forcing period F_5 and shown in dark gray) and the attracting part (shown in black).

We consider a smooth doubled torus with two bands in M, which exists below the basin boundary metamorphosis line. This two-band torus is transformed into a pair of conjugate single-band tori in M^2. Fig. 2(c) shows the conjugate tori (denoted by heavy black lines) inside their absorbing areas bounded by the critical curves L_k $(k = 1, \ldots, 8)$ for $a = 3.46$ and $\varepsilon = 0.11$. The basins of the upper and lower tori are shown in light gray and gray, respectively. However, when passing the basin boundary metamorphosis line, the absorbing areas become broken up through collision with the unstable parent torus (denoted by the dashed line) on a basin boundary. Then, the basin of each torus becomes complex, because it contains "holes" of other basin of the counterpart, as shown in Fig. 2(d) for $a = 3.48$ and $\varepsilon = 0.13$. Due to this basin boundary metamorphosis, the unstable parent torus becomes inaccessible from the interior of the basins of the upper and lower tori, and hence it cannot induce any BM transition. For this case, using the rational approximations to the quasiperiodic forcing, we locate an invariant ring-shaped unstable set that causes a new type of BM transition. When passing the dash-dotted line in Fig. 1, a pair of conjugate ring-shaped unstable sets is born via phase-dependent saddle-node bifurcations in M^2 [17]. This bifurcation has no counterpart in the unforced case. As an example, in the rational approximation of level $k = 5$ we explain the structure of the ring-shaped unstable set. As shown in Fig. 2(e) for $a = 3.396$ and $\varepsilon = 0.146$, the rational approximation to each ring-shaped unstable set, consisting of F_5 $(= 5)$ small rings, exists in the basin of the rational approximation to each smooth torus (denoted by a black curve and composed of stable orbits with period F_5). At first, each ring is composed of the stable (shown in black) and unstable (shown in dark gray) orbits with the forcing period F_5 (see the inset in Fig. 2(e)). However, as the parameters a and ε are increased, these rings evolve, and then each ring consists of a large unstable part (shown in dark gray) and a small attracting part (shown in black) (see the inset in Fig. 2(f)). With increase in the level k of the rational approximation, each ring-shaped unstable set becomes composed of a larger number of rings with a smaller attracting part. Hence, we believe that, in the quasiperiodic limit, the ring-shaped unstable set might become a complicated invariant unstable set consisting of only unstable orbits. Through a collision with this ring-shaped unstable set which has no counterpart in the unforced case, a new type of BM transition occurs, as will be shown below.

As ε is further increased, both the new BM transition curve and the basin boundary metamorphosis line cease simultaneously at the upper double-crisis vertex (denoted by a plus) $(a_u^*, \varepsilon_u^*) \simeq (3.404, 0.163)$ in Fig. 1(a). Then, the standard BM transition line, which is connected smoothly with the basin boundary metamorphosis line at the upper vertex, begins again by making an angle. Along the routes α, β, and γ beyond the upper vertex, standard BM transitions of a chaotic attractor, SNA, and smooth torus occur, respectively, through a collision with the smooth unstable torus. On the other hand, the new BM transition curve transforms smoothly to a curve of intermittency at the upper vertex. When passing the intermittency line (route a in Fig. 1(b)), a transition from a smooth two-band torus to an intermittent two-band SNA occurs through collision with a ring-shaped unstable set [17]. As in the case of interior crisis (route b Fig. 1(b)), the size of the attractor abruptly increases (without band merging). Hereafter, we will investigate the new BM transitions which occur along the routes A, B, and C crossing the segment bounded by the two double-crisis vertices (see Fig. 1(b)). A new BM transition is found to take place for a nonchaotic attractor (smooth torus (route A) and SNA (route B)) as well as a chaotic attractor (route C) through a collision with a ring-shaped unstable set. Particularly, a single-band SNA appears as a result of the new BM transition of a two-band smooth torus.

We now fix the value of a at $a = 3.43$ and study the BM transition from a two-band torus to a single-band intermittent SNA by varying ε along the route A. A two-band torus in the original map M is transformed into a pair of conjugate tori in M^2. Fig. 3(a) shows a pair of upper and lower tori (denoted by black curves) for $\varepsilon = 0.161$, whose basins are shown in light gray and gray, respectively. For this case, the basin of each smooth torus contains holes of other basin of the counterpart. Hence, the smooth unstable torus (denoted by the dashed line) is not accessible from the interior of the basins of the conjugate (attracting) tori. As the parameter ε increases, conjugate tori and holes become closer. Eventually, for $\varepsilon = \varepsilon^*$ $(= 0.161\,323\,479)$ an attractor-merging crisis of the conjugate tori occurs through a collision with a hole boundary, and

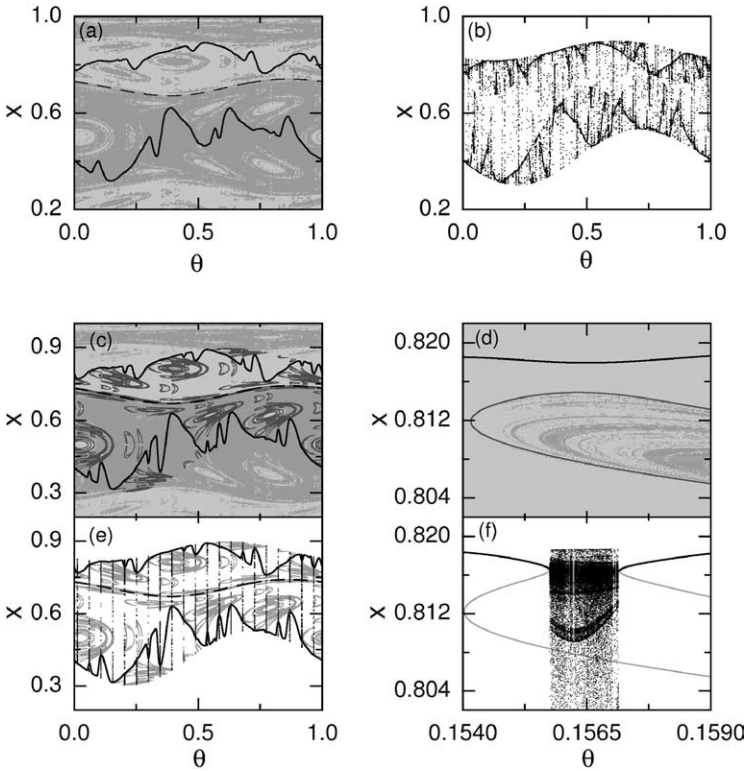

Fig. 3. BM transition of a two-band torus for $a = 3.43$. There exists a pair of conjugate tori in M^2, which are denoted by black lines in (a) for $\varepsilon = 0.161$. The basins of the upper and lower tori are shown in light gray and gray, respectively. Each basin is complex, because it contains holes of other basin of the counterpart. Through a collision with a hole boundary, the conjugate tori merge into a single-band SNA, as shown in (b) for $\varepsilon = 0.163$. (c)–(f) Analysis of the mechanism for the BM transition of the two-band torus for $a = 3.43$, using the rational approximation of level 8. In (c), the eight rational approximation to the conjugate tori and ring-shaped unstable sets are plotted in M^2 for $\varepsilon = 0.1597$. For this case, the ring-shaped unstable sets (represented by dark gray curves), some part of which exists on a hole boundary, lie close to the smooth tori (denoted by black lines) (e.g., see a magnified view in (d), where holes in the light gray basin are denoted by gray dots). Through collision between the smooth tori and the ring-shaped unstable sets, F_8 $(= 21)$ "gaps", filled by single-band intermittent chaotic attractors denoted by black dots, are formed, as shown in (e) for $\varepsilon = 0.15976$. For a clear view, a magnified gap is given in (f). In (e) and (f), attractors (denoted by black dots) and ring-shaped unstable sets (represented by gray curves) are plotted in the original map M.

then for $\varepsilon = 0.163$, a single-band intermittent SNA with $\sigma_x = -0.019$ and $\delta = 10.8$ appears in M, as shown in Fig. 3(b). Using the rational approximation of level $k = 8$, we investigate the mechanism for the BM transition of the smooth torus. Fig. 3(c) shows conjugate tori (denoted by black lines), conjugate ring-shaped unstable sets (represented by dark gray lines), and holes (shown in gray and light gray inside the basins of the upper and lower tori, respectively) in M^2 for $\varepsilon = 0.1597$. The rational approximations to the smooth torus and the ring-shaped unstable set are composed of stable and unstable orbits with period F_8 $(= 21)$, respectively. For this case, some part of each ring-shaped unstable set (denoted by dark gray curves) lies on a hole boundary (e.g., see a magnified view in Fig. 3(d), where holes in the light gray basin are represented by gray dots). With increase in ε, the conjugate tori and ring-shaped unstable sets become closer, and eventually, for $\varepsilon = \varepsilon_8^*$ $(= 0.159\,750\,121)$ a pair of phase-dependent saddle-node bifurcations occurs through collision between the conjugate tori and ring-shaped unstable sets. Then, F_8 $(= 21)$ "gaps", where no orbits with period F_8 exist, are formed in the whole range of θ, as shown in Fig. 3(e) for $\varepsilon = 0.15976$. In these gaps, single-band intermittent chaotic attractors (denoted by black dots) appear (i.e., saddle-node bifurcations induce attractor-merging crises in the gaps) (for a clear view, a magnified gap is given in Fig. 3(f)).

Thus, the rational approximation to the whole attractor in the original map M becomes composed of the union of the two-band periodic component and the single-band intermittent chaotic component. Since the periodic component is dominant, the average Lyapunov exponent ($\langle\sigma_x\rangle = -0.105$) is negative, where $\langle\cdots\rangle$ denotes the average over the whole θ. Hence, the (partially-merged) 8th rational approximation to the attractor in Fig. 3(e) becomes nonchaotic, and resembles the single-band SNA in Fig. 3(b), although the level $k = 8$ is low. By increasing the level of the rational approximation to $k = 16$, we study the BM transition of the two-band torus. It is thus found that the threshold value ε_k^*, at which the phase-dependent saddle-node bifurcation of level k (inducing attractor-merging crises in the gaps) occurs, converges to the quasiperiodic limit ε^* ($= 0.161\,323\,479$) in an algebraic manner, $|\Delta\varepsilon_k| \sim F_k^{-\alpha}$, where $\Delta\varepsilon_k = \varepsilon_k^* - \varepsilon^*$ and $\alpha \simeq 2.0$. As the level k of the rational approximation increases, the number of gaps, where phase-dependent attractor-merging crises occur, becomes larger, and eventually in the quasiperiodic limit, the rational approximation to the attractor has a dense set of gaps, filled by single-band intermittent chaotic attractors. Consequently, an intermittent single-band SNA, containing the ring-shaped unstable set, appears, as shown in Fig. 3(b). We note that this transition from a two-band torus to a single-band intermittent SNA corresponds to a new mechanism for the appearance of SNAs.

The intermittent SNA, born via attractor-merging crisis [23], may be characterized in terms of the average time between bursts and the local Lyapunov exponents [13–15]. A typical trajectory of the second iterate of Eq. (1) (i.e., M^2) spends a long stretch of time in the vicinity of one of the two former attractors (i.e., smooth tori), then it bursts out from this region and comes close to the same or other former tori where it remains again for some time interval, and so on. In this way the trajectory irregularly jumps between the two former tori. For this case, the characteristic time τ is the average over a long trajectory of the time between bursts (i.e., jumps) [23]. As shown in Fig. 4(a) for $a = 3.43$, the average value of τ exhibits a power-law scaling behavior,

$$\langle\tau\rangle \sim (\varepsilon - \varepsilon^*)^{-\gamma}, \quad \gamma = 0.5 \pm 0.002. \tag{2}$$

The scaling exponent γ is the same as that for the case of the intermittent route to SNAs occurring near the main tongue of the quasiperiodically forced logistic map [13]. Since the dynamical mechanisms for the appearance of intermittent SNAs near the main tongue [17] and the second-order tongue (in the present case) are the same (i.e., an intermittent SNA appears via a phase-dependent saddle-node bifurcation between a smooth torus and a ring-shaped unstable set), the intermittent SNAs for both cases seem to exhibit the same scaling behaviors. Fig. 4(b) shows the plot of the Lyapunov exponent σ_x versus $\Delta\varepsilon$ ($= \varepsilon - \varepsilon^*$). We note that σ_x abruptly increases during the transition from torus to SNA, which is similar to the case of the intermittent route to SNA [13]. We also discuss the distribution of local (M-time) Lyapunov exponents σ_x^M, causing the sensitivity of the SNA with respect to the phase θ of the quasiperiodic forcing [8]. As an example, we consider the case of $a = 3.43$ and $\varepsilon = 0.163$ and obtain the probability distribution $P(\sigma_x^M)$ of local (M-time) Lyapunov exponents σ_x^M by taking a long trajectory dividing it into segments of length M and calculating σ_x^M in each segment. For $M = 100$, 500, and 1000, $P(\sigma_x^M)$'s are shown in Fig. 4(c). In the limit $M \to \infty$, $P(\sigma_x^M)$ approaches the delta distribution $\delta(\sigma_x^M - \sigma_x)$, where σ_x ($= -0.019$) is just the usual averaged Lyapunov exponent. However, we note that the distribution $P(\sigma_x^M)$ has a significant positive tail which does not vanish even for large M. To quantify this slow decay of the positive tail, we define the fraction of positive local Lyapunov exponents as

$$F_M^+ = \int_0^\infty P\left(\sigma_x^M\right) d\sigma_x^M. \tag{3}$$

These fractions F_M^+'s are plotted for $\varepsilon = 0.163$, 0.165, and 0.1667 in Fig. 4(d). Note that for each value of ε, the fraction F_M^+ exhibits a power-law decay,

$$F_M^+ \sim M^{-\eta}. \tag{4}$$

Here the values of the exponent η decreases as ε increases. Consequently, a trajectory on any SNA has segments of arbitrarily long M that have positive local Lyapunov exponents, and thus it has a phase sensitivity, inducing the strangeness of the SNA. As shown in Fig. 4(d), as ε increases the value of F_M^+ becomes larger. Hence, the degree of the phase sensitivity of the SNA increases.

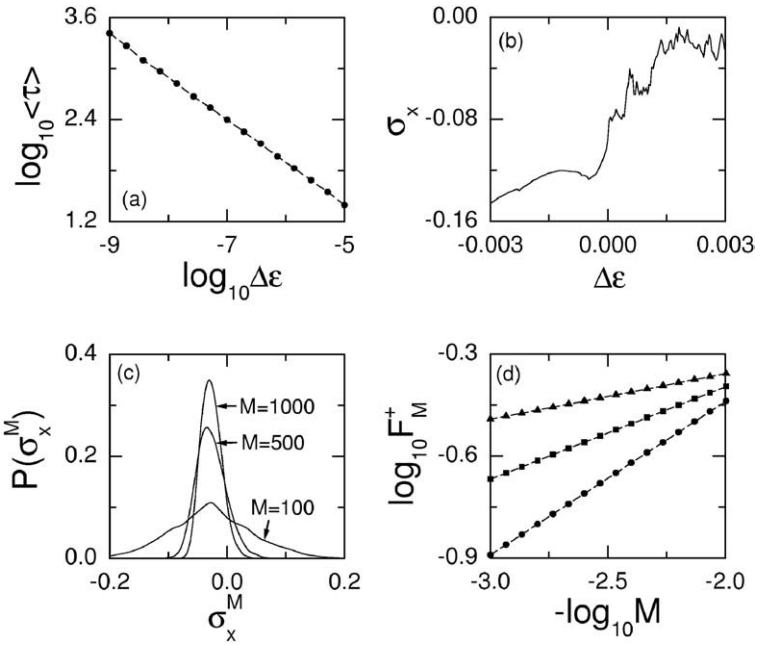

Fig. 4. (a) Plot of $\log_{10}\langle\tau\rangle$ ($\langle\tau\rangle$ is the average time between bursts) versus $\log_{10}\Delta\varepsilon$ ($\Delta\varepsilon = \varepsilon - \varepsilon^*$) for $a = 3.43$. The data are well fitted with the straight line with the slope $\gamma = 0.5 \pm 0.002$. (b) Plot of σ_x versus $\Delta\varepsilon$ for $a = 3.43$. We note that abrupt change in σ_x near the transition point. (c) Three probability distributions $P(\sigma_x^M)$ of the local M-time Lyapunov exponents for $M = 100$, 500, and 1000 when $a = 3.43$ and $\varepsilon = 0.163$. (d) Plots of $\log_{10} F_M^+$ (F_M^+: fraction of the positive local Lyapunov exponents) versus $-\log_{10} M$. Note that the three plots for $\varepsilon = 0.163$ (circles), 0.165 (squares), and 0.1667 (triangles) are well fitted with the straight lines with the slopes $\eta = 0.45$, 0.27, and 0.13, respectively. Hence F_M^+ decays with some power η.

When crossing the remaining part of the new BM transition curve along the route B (C) in Fig. 1(b), a transition from a two-band SNA (chaotic attractor) into a single-band one occurs via a collision with a ring-shaped unstable set. We fix the value of ε at $\varepsilon = 0.1305$ and investigate the BM transition of a two-band SNA by varying a along the route B. For $a = 3.5153$, there exists a two-band SNA with $\sigma_x = -0.027$ and $\delta = 1.752$ in the original map M. This two-band SNA is transformed into a pair of conjugate SNAs in M^2, which is denoted by black dots in Fig. 5(a). The basins of the upper and lower SNAs are shown in light gray and gray, respectively. For this case, the unstable smooth torus (denoted by a dashed line) is not accessible from the interior of the basins of the conjugate SNAs, because the basin of each SNA contains holes of other basin of the counterpart. As a is increased, conjugate SNAs and holes become closer. Eventually, an attractor-merging crisis of the conjugate SNAs occurs for $a = a^*$ ($= 3.515\,342\,763$) through a collision with a hole boundary, and then for $a = 3.5157$, a single-band SNA with $\sigma_x = -0.013$ and $\delta = 3.734$ appears in M, as shown in Fig. 5(b). As in the case of the SNA, BM transition of a chaotic attractor also occurs along the route C through a collision with a hole boundary. For example, at a fixed value of $\varepsilon = 0.105$, we consider a two-band chaotic attractor with $\sigma_x = 0.023$ in M for $a = 3.535$. This two-band chaotic attractor turns into a pair of conjugate single-band chaotic attractors in M^2, which is represented by black dots in Fig. 5(c). An attractor-merging crisis of the upper and lower chaotic attractors takes place when passing a threshold value of $a = 3.538\,034\,276$, and then for $a = 3.545$, a single-band chaotic attractor with $\sigma_x = 0.077$ appears in M, as shown in Fig. 5(d). Since the mechanism for the BM transition of the chaotic attractor is the same as that for the case of the SNA, it is sufficient to consider only the case of the SNA for presentation of the mechanism for the BM transition. Hence, using the rational approximation of level $k = 8$, we investigate the mechanism for the BM transition of the SNA along the route B for $\varepsilon =$

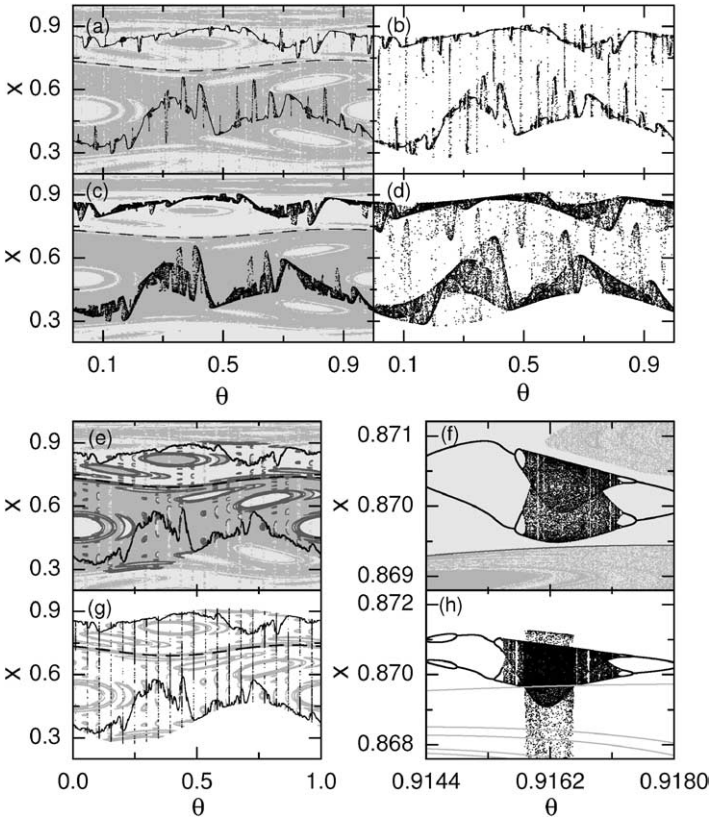

Fig. 5. (a) and (b) BM transition of a two-band SNA for a fixed value of $\varepsilon = 0.1305$. A pair of conjugate SNAs in M^2 is represented by black dots in (a) for $a = 3.5153$. The basins of the upper and lower SNAs are shown in light gray and gray, respectively. Due to a collision with a hole boundary, the conjugate SNAs merge to form a single-band SNA, as shown in (b) for $a = 3.5157$. (c) and (d) BM transition of a two-band chaotic attractor for a fixed value of $\varepsilon = 0.105$. A pair of conjugate chaotic attractors in M^2 is denoted by black dots in (c) for $a = 3.535$. The basins of the upper and lower chaotic attractors are shown in light gray and gray, respectively. Because of a collision with a hole boundary, the upper and lower chaotic attractors merge to form a single-band chaotic attractor, as shown in (d) for $a = 3.545$. (e)–(h) Investigation of the mechanism for the BM transition of the SNA in the rational approximation of level $k = 8$ for $\varepsilon = 0.1305$. The rational approximations to the conjugate SNAs and the conjugate ring-shaped unstable sets in M^2 are denoted by black dots and dark gray curves, respectively, in (e) for $a = 3.5224$. Some part of the ring-shaped unstable set, represented by dark gray lines, lies on a hole boundary (e.g., see a magnified view in (f), where holes in the light gray basin are denoted by gray dots). Through collision between the chaotic components of the rational approximations to the conjugate SNAs and the conjugate ring-shaped unstable sets, F_8 $(= 21)$ "gaps", filled by single-band intermittent chaotic attractors, are formed, as shown in (g) for $a = 3.5229$ (for a clear view, see a magnified gap in (h)). In (g) and (h), attractors (denoted by black dots) and ring-shaped unstable sets (represented by gray curves) are plotted in the original map M.

0.1305. Fig. 5(e) and (f) show the rational approximations to the conjugate SNAs (denoted by black dots) and conjugate ring-shaped unstable sets (represented by dark gray curves) for $a = 3.5224$. For this case, the rational approximation to a SNA is composed of periodic and chaotic components, and some part of the ring-shaped unstable set (denoted by dark gray lines) lies on a hole boundary (e.g., see a magnified view in Fig. 5(f), where holes in the light gray basin are denoted by gray dots). As a is increased, the chaotic components of the rational approximations to the conjugate SNAs and the conjugate ring-shaped unstable sets on the hole boundary become closer. Eventually, for $a = a_8^*$ $(= 3.522\,675\,762)$, they make a collision and then a phase-dependent attractor-merging crisis occurs. Thus, F_8 $(= 21)$ "gaps", filled by single-band intermittent chaotic attractors (represented by black dots), are formed in the whole range of θ, as shown in Fig. 5(g) for $a = 3.5229$ (for a clear view, a magnified gap is given in Fig. 5(h)). This (partially-merged) ra-

tional approximation to the attractor, composed of the union of the periodic and chaotic components, has a negative average Lyapunov exponent ($\langle\sigma_x\rangle = -0.046$ in M), because its periodic component is dominant. Hence, the 8th rational approximation to the attractor in Fig. 5(g) becomes nonchaotic, and is similar to the single-band SNA in Fig. 5(b). Increasing the level of the rational approximation to $k = 16$, we find that the threshold value a_k^*, at which the phase-dependent attractor-merging crisis of level k occurs, converges to the quasiperiodic limit a^* ($= 3.515\,342\,763$) in an algebraic manner, $|\Delta a_k| \sim F_k^{-\alpha}$, where $\Delta a_k = a_k^* - a^*$ and $\alpha \simeq 2.8$. In the quasiperiodic limit $k \to \infty$, there appear a dense set of gaps, filled by single-band intermittent chaotic attractors, in the rational approximation to the attractor. Consequently, when passing the threshold value a^* along the route B, a transition from a two-band SNA to an intermittent single-band SNA, containing the ring-shaped unstable set, occurs.

3. Summary

We have investigated the mechanism for the BM transitions in the quasiperiodically forced logistic map which is a representative model for quasiperiodically forced period-doubling systems. Using the rational approximations to the quasiperiodic forcing, a new type of BM transition is found to occur for a nonchaotic attractor (smooth torus or SNA) as well as a chaotic attractor via a collision with an invariant ring-shaped unstable set which has no counterpart in the unforced case. Particularly, a single-band intermittent SNA appears via a new BM transition of a two-band smooth torus, which corresponds to a new mechanism for the birth of SNAs. Characterization of the intermittent SNA has also been made in terms of the average time between bursts and the local Lyapunov exponents. This kind of new BM transition is in contrast to the standard BM transition which takes place through a collision with the smooth unstable torus. Finally, we note that the new BM transition seems to be "universal", in the sense that it occurs via the same mechanism in typical quasiperiodically forced period-doubling systems of different nature, such as the quasiperiodically forced Hénon map and Toda oscillator [20].

Acknowledgement

This work was supported by the 2004 Research Program of the Kangwon National University.

References

[1] E. Ott, Chaos in Dynamical Systems, Cambridge Univ. Press, Cambridge, 2002.
[2] M.J. Feigenbaum, J. Stat. Phys. 19 (1978) 25.
[3] E.N. Lorentz, Ann. N.Y. Acad. Sci. 357 (1980) 282.
[4] A. Prasad, S.S. Negi, R. Ramaswamy, Int. J. Bifurc. Chaos 11 (2001) 291.
[5] C. Grebogi, E. Ott, S. Pelikan, J.A. Yorke, Physica D 13 (1984) 261.
[6] F.J. Romeiras, E. Ott, Phys. Rev. A 35 (1987) 4404;
M. Ding, C. Grebogi, E. Ott, Phys. Rev. A 39 (1989) 2593.
[7] J.F. Heagy, S.M. Hammel, Physica D 70 (1994) 140.
[8] A.S. Pikovsky, U. Feudel, Chaos 5 (1995) 253. See Eqs. (11)–(14) for the definition of the phase sensitivity exponent δ.
[9] O. Sosnovtseva, U. Feudel, J. Kurths, A. Pikovsky, Phys. Lett. A 218 (1996) 255.
[10] S.P. Kuznetsov, A.S. Pikovsky, U. Feudel, Phys. Rev. E 51 (1995) R1629;
S. Kuznetsov, U. Feudel, A. Pikovsky, Phys. Rev. E 57 (1998) 1585.
[11] T. Nishikawa, K. Kaneko, Phys. Rev. E 54 (1996) 6114.
[12] T. Yalçınkaya, Y.-C. Lai, Phys. Rev. Lett. 77 (1996) 5039.
[13] A. Prasad, V. Mehra, R. Ramaswamy, Phys. Rev. Lett. 79 (1997) 4127;
A. Prasad, V. Mehra, R. Ramaswamy, Phys. Rev. E 57 (1998) 1576.
[14] A. Witt, U. Feudel, A. Pikovsky, Physica D 109 (1997) 180.
[15] A. Venkatesan, K. Murali, M. Lakshmanan, Phys. Lett. A 259 (1999) 246;
A. Venkatesan, M. Lakshmanan, A. Prasad, R. Ramaswamy, Phys. Rev. E 61 (2000) 3641;
A. Venkatesan, M. Lakshmanan, Phys. Rev. E 63 (2001) 026219.
[16] B.R. Hunt, E. Ott, Phys. Rev. Lett. 87 (2001) 254101;
J.-W. Kim, S.-Y. Kim, B. Hunt, E. Ott, Phys. Rev. E 67 (2003) 036211.
[17] S.-Y. Kim, W. Lim, E. Ott, Phys. Rev. E 67 (2003) 056203;
S.-Y. Kim, W. Lim, J. Phys. A 37 (2004) 6477.
[18] W.L. Ditto, M.L. Spano, H.T. Savage, S.N. Rauseo, J. Heagy, E. Ott, Phys. Rev. Lett. 65 (1990) 533;
T. Zhou, F. Moss, A. Bulsara, Phys. Rev. A 45 (1992) 5394;
W.X. Ding, H. Deutsch, A. Dinklage, C. Wilke, Phys. Rev. E 55 (1997) 3769;
T. Yang, K. Bilimgut, Phys. Lett. A 236 (1997) 494;
B.P. Bezruchko, S.P. Kuznetsov, Y.P. Seleznev, Phys. Rev. E 62 (2000) 7828.
[19] C. Grebogi, E. Ott, J.A. Yorke, Phys. Rev. Lett. 56 (1986) 1011;
C. Grebogi, E. Ott, J.A. Yorke, Physica D 24 (1987) 243;
U. Feudel, A. Witt, Y.-C. Lai, C. Grebogi, Phys. Rev. E 58 (1998) 3060.

[20] W. Lim, S.-Y. Kim, unpublished.
[21] C. Mira, L. Gardini, A. Barugola, J.-C. Cathala, Chaotic Dynamics in Two-Dimensional Noninvertible Maps, World Scientific, Singapore, 1996.
[22] J.A. Gallas, C. Grebogi, J.A. Yorke, Phys. Rev. Lett. 71 (1993) 1359;
H.B. Stewart, Y. Ueda, C. Grebogi, J.A. Yorke, Phys. Rev. Lett. 75 (1995) 2478.
[23] C. Grebogi, E. Ott, F. Romeiras, J.A. Yorke, Phys. Rev. A 36 (1987) 5365.